

## NUMERICAL SIMULATION OF MASS DIFFUSION IN BRAIN TISSUES

Adrian Neculae<sup>1</sup> and Dan Curticapean<sup>2</sup>

<sup>1</sup>*Faculty of Physics, West University Timisoara, Bly. V. Parvan No. 4, 300223 Timisoara, Romania*

<sup>2</sup>*University of Applied Sciences Offenburg, Badstr. 24, D-77652 Offenburg, Germany*

### Article Info

*Received: 29 December 2010*

*Accepted: 16 January 2011*

### Keywords:

brain-cell microenvironment,  
diffusion equation,  
tortuosity,  
volume fraction,  
porous medium

### Abstract

In the brain-cell microenvironment, in absence of electrical activity inside the cells or without an externally applied electric field, the movement of ions is governed by diffusion. In this complex medium, the primary constraints on long-range diffusion are due to the geometrical properties of the medium, especially tortuosity and volume fraction, which are the most important parameters that incorporate local geometrical properties such as connectivity and pore size. In this paper we present a set of numerical simulations for the evolution of the concentration profile for an injected substance in brain tissues. The computations are performed by solving the diffusion equation in the extracellular space of the tissue, modeled as a porous medium. Three different types of cells are considered and the influence of the geometrical properties is analyzed. This modeling may partially replace the need for some types of diffusion experiments in brain tissue.

### 1. Introduction

Diffusion plays a crucial role in brain function: besides delivering glucose and oxygen from the vascular system to brain cells, it also moves informational substances between cells, a process known as volume transmission. In treating brain disorders, where diffusion is often compromised, understanding the transport of molecules can be crucial to effective drug delivery. The brain is an extremely complex structure of interwoven, intercommunicating cells of about 5–50  $\mu\text{m}$  in diameter, whose functional mechanisms remain largely an enigma, perhaps the last great unknown frontier of medical science [1]. Despite this, it became apparent that the classical laws of diffusion, cast in the framework of porous media theory, can deliver an accurate quantitative description of the way that molecules are transported through this tissue [1-3].

This paper is a numerical study on how substances diffuse through the brain. The diffusion-generated concentration distributions of well-chosen molecules also reveal the structure of brain tissue. This structure is represented by the volume fraction (void space) and the tortuosity (hindrance to diffusion imposed by local boundaries or local viscosity). Analysis of these parameters also reveals how the local geometry of the brain changes with time or under pathological conditions. The numerical simulations concern basically with important biophysical consequences of the packing.

## 2. Theoretical background

Transport phenomena through porous media have been the subject of various studies due to an increasing need for a better understanding of the associated transport processes. The brain contains a complicated network of specialized cells called neurons (or nerve cells) and glia (glial cells), each of which is bounded by a thin membrane. The membrane separates the brain into two compartments: extracellular space (ECS), consisting of narrow spaces between cellular elements which constitute the brain-cell microenvironment, and intracellular space (ICS). From the perspective of the transport equations, the densely packed cells of the brain and their interstitial spaces can be regarded as resembling a porous medium with two phases, one permeant and one impermeant. The interstitial spaces remain open under most conditions and the ECS, from a topological viewpoint, is a multiply connected three-dimensional domain. The principle of averaging method used in obtaining the transport equation in porous media is sketched in Fig. 1.

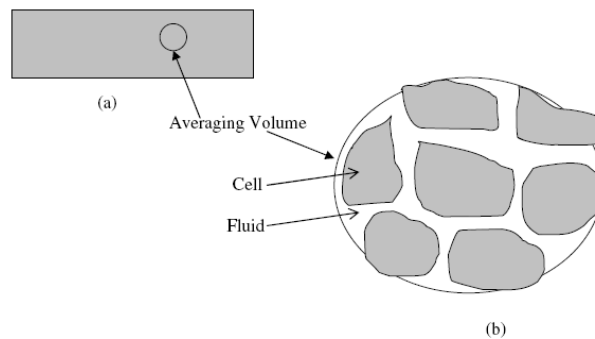


**Figure 1.** The principle of averaging method (a) macroscopic view, (b) microscopic view.

The averaged mass diffusion equation is [1]:

$$\frac{\partial C}{\partial t} = D^* \nabla^2 C + \frac{S}{\varepsilon} \quad (1)$$

where we noted  $D^* = \frac{D}{\lambda^2}$ ,  $D$  - the diffusivity in pure fluid,  $D^*$  - effective diffusivity in porous medium,  $\lambda$  - tortuosity,  $t$  - time,  $C$  - concentration of species,  $\varepsilon$  - volume fraction (porosity) and  $S$  - source term.

Volume fraction  $\varepsilon$ , also called the void fraction or porosity, is the ratio of the volume of the ECS to total volume in a suitable representative elementary volume (REV). The value can take the range  $0 < \varepsilon < 1$  and  $\varepsilon$  is often expressed as a percentage. The effect of  $\varepsilon < 1$  on a source that releases molecules at a constant rate is that local concentration of molecules in the vicinity of the source will be higher than in a free medium because there is less volume to accommodate them.

The tortuosity is defined by  $\lambda = \sqrt{D/D^*}$ . This formal definition is unambiguous and, from an operational standpoint, means that the investigator determines the diffusion coefficient  $D$ , for a suitable molecule, in a free medium (water or dilute gel) and compares it with the diffusion coefficient  $D^*$  determined using the same molecule in the brain.  $\lambda$  is the factor by which the distance the substance has to travel between the outer surface and any point inside is increased by reason of obstacles. It is usually true that  $D^* < D$  so  $\lambda > 1$ ; Diffusion is ‘slower’ in the brain compared to a free medium because the diffusing molecules are ‘hindered’ in the convoluted spaces of the ECS.

Before the substance can be detected it must be released. The simplest approach for the source term is to fill a micropipette with an appropriate solution, at a concentration  $C_0$ , and apply a brief pulse of inert gas (typically  $N_2$ ) to the back end of the barrel. This results in the release a small volume,  $U$ , of substance that approximates a  $\delta$ -function in both space and time; then the amount released,  $N$ , will be  $N = UC_0$ . In the case of homogeneous medium with spherical symmetry, equation (1) has analytical solution. The concentration that can be measured at a distance  $r$  from the source at a moment of time  $t$  is:

$$C(r,t) = \frac{UC_0}{\varepsilon} \frac{\lambda^3}{(4\pi Dt)^{3/2}} \exp\left(-\frac{\lambda^2 r^2}{4Dt}\right) \quad (2)$$

By suitable curve fitting procedures, one can extract two composite parameters:

$$A = \frac{UC_0}{\varepsilon} \frac{\lambda^3}{(4\pi D)^{3/2}} \text{ and } B = \frac{\lambda^2 r^2}{4D}. \text{ The values of } r, D \text{ and } C_0 \text{ are usually known, so } \lambda \text{ can be}$$

determined from  $B$ , but because  $U$  is hard to determine, only the ratio  $U/\varepsilon$  is available from  $A$ .

Frequently, the volume injected,  $U$ , is not confined to a point but fills a finite volume of the tissue. Assuming that the injected material infiltrates the ECS (experimental work supports this assumption) then, the radius  $b$  of the material in the tissue is given by  $b=(3U/4\pi\varepsilon)^{1/3}$  [1]. Curve fitting can extract  $b$  and  $\lambda$  but again, knowledge of  $b$  only provides the ratio  $U/\varepsilon$ .

It can be shown by numerical evaluation of equation (1) with realistic parameters that usually it holds only when  $r > 2b$ . If it is believed that the injected material forms a cavity and in this case a numerical solution is required [1]. In the next section we present a set of numerical simulations concerning the concentration profile evolution for three types of idealized cells, considering two possible injection mechanisms.

### 3. Numerical results

The concentration fields were obtained by solving equation (1) using a code based on finite element method, FreeFEM [5]. The 3-D computational domain, presented in Figure 2, is a sphere of radius  $R$  containing around its center  $O$  a smaller spherical region of radius  $R_i$  where the injected material is delivered. In all computations we considered  $R \gg R_i$ , and consequently the concentration is considered zero on the outer boundary of the domain.

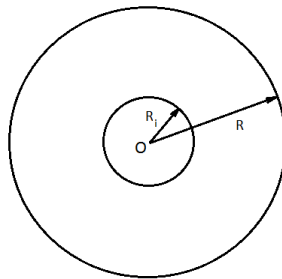


**Figure 2.** Axial section of the spherical computational domain.

Two types of injection source were considered: the case when the injected substance forms a spherical cavity (Figure 3.A) and the case when the injected substance is confined to the pore space (Figure 3.B).

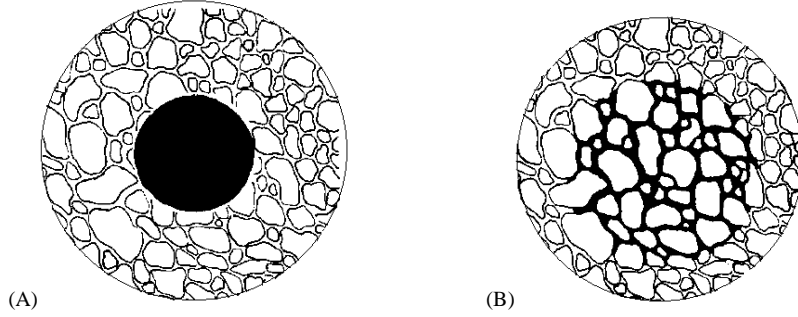


**Figure 3.** Models of injection source; (A) The injected substance forms a spherical cavity, (B) The injected substance is confined to the pore space.

We note that if the same volume of substance,  $V_0$ , is injected in the tissue, the radius of the source term will have the value  $R_a = \sqrt[3]{3V_0 / 4\pi}$  for the mechanism (A), while for the mechanism (B) the radius will be  $R_b = \sqrt[3]{3V_0 / 4\pi\varepsilon} = R_a / \sqrt[3]{\varepsilon} > R_a$ .

The computations were performed for three different idealized cell configurations, for which the tortuosity versus diffusion coefficient variation was reported [4]. The three types of cells are presented, together with their characteristics, in Figure 4.

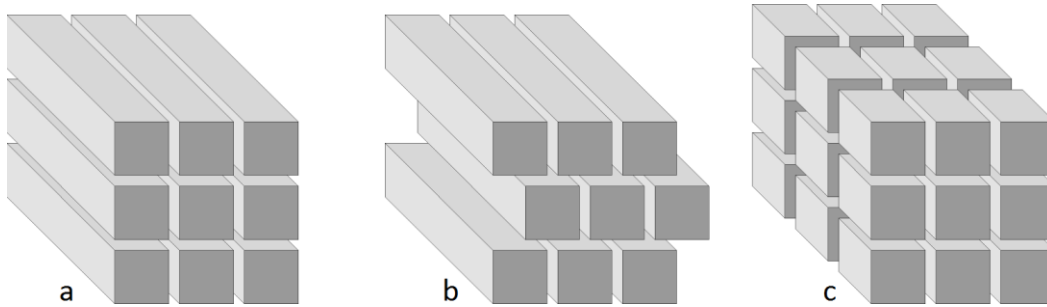


**Figure 4.** Schematic 3-D structures used in computations a) Type 1:  $\varepsilon=0.2166$ ,  $\lambda=1.25$  b) Type 2:  $\varepsilon=0.3$ ,  $\lambda=2.4$ , c) Type 3:  $\varepsilon=0.2$ ,  $\lambda=2.1$

Figures 5a-c present the calculated time evolution of concentration as a function of distance from center of cavity, when the injection is of type (A) for the three types of schematic cells. As in [1], in each considered case, 10 nL of a substance with  $D = 8.7 \times 10^{-6} \text{ cm}^2/\text{s}$  is considered to be instantaneously injected into the brain to form a cavity of 134  $\mu\text{m}$  radius. Initial concentration in cavity is 10 (arbitrary units) and brain tissue around the cavity is characterized by the values of porosity and tortuosity mentioned in Figure 2. Within cavity  $\varepsilon = \lambda = 1$ . Each curve represents concentration as a function of distance from centre of cavity at a succession of 10 s.

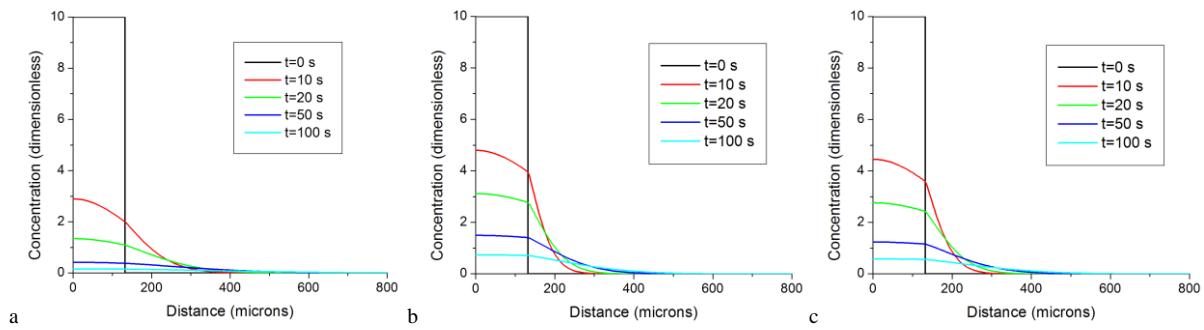


**Figure 5.** Time evolution of concentration as a function of distance from center of cavity when the injection is of type (a) for the three types of schematic cells.

The same type of dependencies, but in the case of an injection of type (B), is depicted in Figures 6a-c. The same volume of substance injected as in (A), but it is now confined to the pore space and so initial radius will modify, according to the corresponding porosity value.

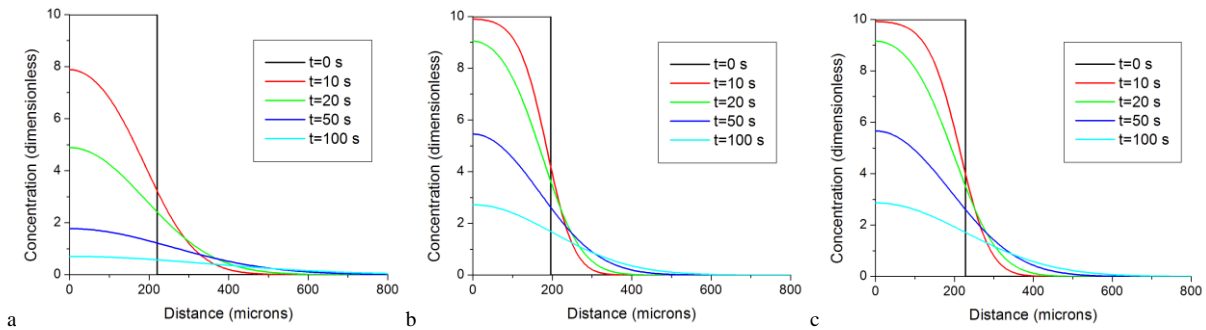


**Figure 6.** Time evolution of concentration as a function of distance from center of cavity when the injection is of type (b) for the three types of schematic cells.

A comparison of concentration profiles at three different time values,  $t = 10, 50$  and  $100$  s, for an injection of type (B) is presented in Figures 7a-c. The type of comparison between the concentration profiles at the same moment of time gives a better image of the influence of cell parameters on the transport inside the brain tissue.

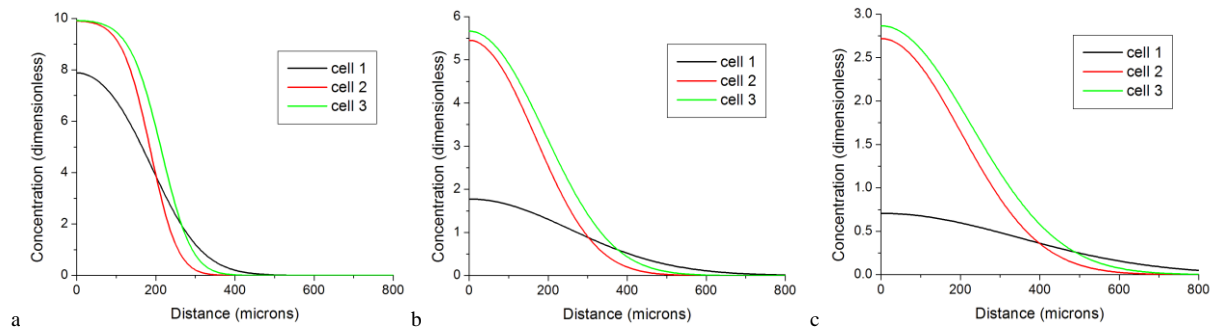


**Figure 7.** Comparison of concentration profiles at three different time values  $t = 10, 50$  and  $100$  s. In the case of a (b)-type injection.

## Conclusions

Brain tissues can be treated in a very good approximation as a porous medium for describing the transport of drugs and nutrient substances. The mathematical modelisation and the numerical simulations are successfully applied in the investigation of diffusion processes in tissues, replacing the costly laboratory investigations. This paper presents a set of computations concerning the mass transport inside the brain tissue, for different types of idealized cells. By measuring the time evolution of the concentration profile of an injected substance and using suitable fitting procedures, the main parameters (tortuosity, volume fraction) which characterize the tissue can be determined and analyzed.

## References

1. C. Nicholson , Rep. Prog. Phys. **64** (2001) 815
2. A. W. El-Kareh, S. L. Braunstein, T. W. Secomb, Biophys. J. **64** (1993) 1638
3. A. R. A. Khaled, K. Vafai, Int. J. Heat Mass Transfer **46** (2003) 4989
4. L. Dai, R. Miura, Siam J. Appl. Math. **59** (1999) 2247
5. [www.freefem.org](http://www.freefem.org)